メタン水蒸気改質における２種類の水素選択透過膜反応器の実験的及び理論的比較

相原雅彦、竹内隆、羽深等

横浜国立大学大学院　工学研究院　機能の創生部門　過程の機能と安全分野

化学システム工学コース

〒240-8501　横浜市保土ヶ谷区常盤台 79-5

Experimental and Theoretical Comparison of Two Types of Hydrogen-Permselective Membrane Reactor for Methane Steam Reforming

Masahiko Aihara, Takashi Takeuchi, Hitoshi Habuka

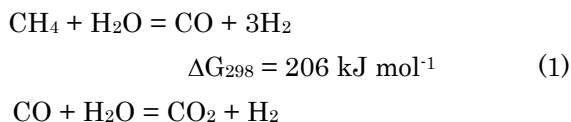[a]Department of Chemical Engineering Science, Yokohama National University

79-5 Tokiwadai, Hodogaya-ku, Yokohama 240-8501, Japan

To compare the experimental data of the membrane reactors with results of simulation, two types of hydrogen-permselective membranes, ZrO_2/SiO_2 composite membrane and Pd membrane, were prepared and installed in a reactor for methane steam reforming, respectively. Hydrogen permeation mechanisms through ZrO_2/SiO_2 composite membrane indicated Knudsen diffusion and that through Pd membrane indicated solution diffusion transport. Comparison with the experimental and simulation data showed a good agreement. The results of numerical analysis based on the obtained exergy of product and the total exergy supplied in the reaction system showed that the exergy loss of hydrogen production using a hydrogen-permselective membrane reactor for methane steam reforming process at the lowest was 30-50% less than that of a conventional process.
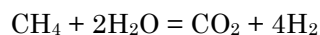
Key words: steam reforming, hydrogen, membrane reactor, exergy analysis

1. Introduction

Methane steam reforming is one of the most important chemical processes in hydrogen production. Methane steam reforming involves five species in two reversible reaction.

$$CH_4 + H_2O = CO + 3H_2$$
$$\Delta G_{298} = 206 \text{ kJ mol}^{-1} \quad (1)$$
$$CO + H_2O = CO_2 + H_2$$
$$\Delta G_{298} = \text{-}41 \text{ kJ mol}^{-1} \quad (2)$$
$$CH_4 + 2H_2O = CO_2 + 4H_2$$
$$\Delta G_{298} = 165 \text{ kJ mol}^{-1} \quad (3)$$

Reaction (1), reforming reaction, is thermodynamically favored by high temperature and low pressure. Reaction (2), water-gas shift, does not depend on pressure and is favored by low temperature. Reaction (3) is the overall reaction.

The conventional industrial process is carried

out in furnace containing hundreds of tubes packed with a catalyst. One possible way to liberate this reaction from the equilibrium limitation and thus attain a high methane conversion is by use of membrane reactor. By employing a hydrogen-permselective membrane, the hydrogen produced by methane steam reforming is removed from the reaction zone so that the chemical equilibrium shifts towards a higher reactant conversion. Based on this concept, hydrogen-permselective membrane reactors have been proposed and investigated for the methane steam reforming process.[1-5]

This paper describes the preparation of two types of hydrogen-permselective membrane and the experimental and numerical analysis of membrane reactor installed these membrane in.

2. Experimental

2.1 Membrane

Two kinds of hydrogen-permselective membrane were prepared and installed in a membrane reactor for methane steam reforming. The former is the ZrO_2/SiO_2 composite membrane expected to be high thermal stability. The later is the Pd membrane well-known for the the high hydrogen-permselectivity.

Via a metal-alkoxide method[4], a thin layer of the ZrO_2/SiO_2 composite membrane was coated on the surface of porous ceramic tubing, the dimensions of which were 10 mm in outer diameter, 7 mm in inner diameter, and the average pore diameter was 100 nm (supplied by NGK INSULATORS. LTD.) The composition of the coating solutions are listed on Table 1 and the procedure of preparing the composite membrane is outlined in Fig. 1(a).

The Pd membrane was coated on the surface of the same porous ceramic tubing by the electroless-plating method[5-7]. The base ceramic tubing was sensitized and activated by

pretreatment with aqueous solutions of stannous chloride and palladium chloride, respectively. The composition of the plating solutions are listed on Table 2 and the procedure of preparing the Pd membrane is outlined in Fig. 1(b).
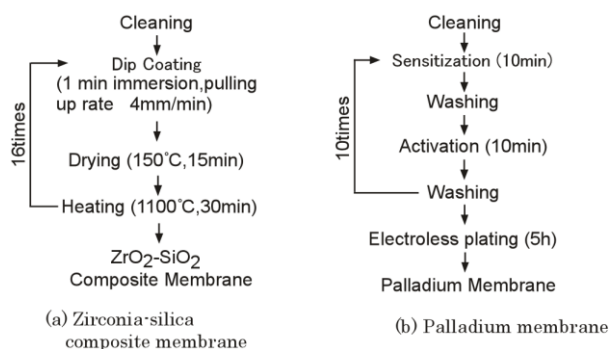

Fig. 1. Preparation of separation membrane

Table 1. Coating solution for Alkoxide method

$Zr(OC_3H_7)_4$	22.4 ml
$Si(OC_2H_5)_4$	0.9 ml
$Y(CH_3COO)_3 \cdot 4H_2O$	1.0 g
$i\text{-}C_3H_7OH$	84.8 ml

Table 2. Electroless-plating solution

$Pd[(NH_3)_4]Cl_2$	4.7 g
$EDTA \cdot 2Na$	67.2 g
NH_3 (28% solution)	651.3 ml
H_2NNH_2	0.35 ml
H_2O	348.4 ml

2.2 Apparatus

A schematic flow diagram of the experimental apparatus is shown in Fig. 2. A schematic view of the reactor cell is shown in Fig. 3. For the measurement of membrane separation characteristic, no catalyst is packed in the reactor cell. For the investigation of reaction characteristic, Ru/Al_2O_3 catalyst pellets and alumina balls were packed in the annular region between two coaxial circular cylinders by the length of effective membrane. The inner cylinder which is perforated with circular holes of 2 mm, and of 22 % open area ratio, protects the active

surface of the membrane from the direct contact with catalyst pellets. The Ru-catalyst which is the alumina cylinder pellet containing 0.5% ruthenium (D: 3.2 mm, L: 3.4 mm, Pore Volume: 0.33-0.37 cm³/g, Superficial Density: 1.55 g/cm³; N. E. Chemcat, Co. Ltd.) is used for steam reforming reaction experiment. The catalyst concentration and the height of catalyst zone are adjusted using alumina balls (D: 3.2 mm, Superficial Density: 3.45 g/cm³). The flexible heaters were used to avoid the condensation of water contained in the reacted gas mixtures in the tubing of which temperature was kept above 423 K.
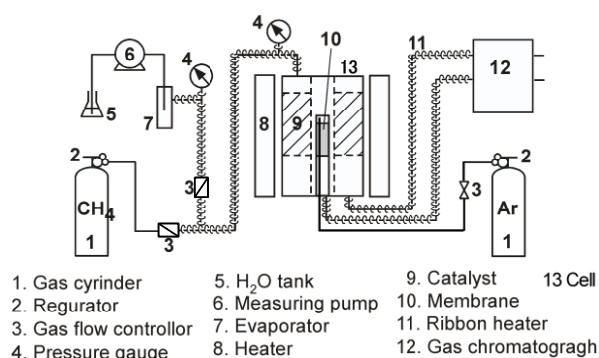

1. Gas cyrinder
2. Regurator
3. Gas flow controllor
4. Pressure gauge
5. H₂O tank
6. Measuring pump
7. Evaporator
8. Heater
9. Catalyst
10. Membrane
11. Ribbon heater
12. Gas chromatogragh
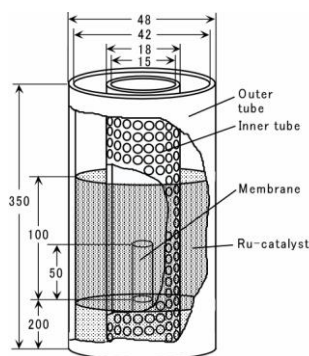13 Cell

Fig. 2. Experimental apparatus

Fig. 3. Reactor Cell

2.3 Evaluation of membrane performance

Pure gas permeations of ZrO_2/SiO_2 composite membrane and Pd membrane were evaluated, respectively. Each feed pure gas of H_2, CO_2 and CH_4 was introduced from each gas cylinder into the cell. In the case of measurement of water vapor permeation through the membrane, water was introduced by the measuring pump into the evaporator where it was vaporized, and introduced into the cell. Ar gas was introduced onto the surface of the permeation side of membrane to purge the permeant. The pressure in the cell was controlled by the pressure-control valve. The water vapor permeation rate through the membrane was determined by the weight method, using cold trap cooled by liquid N_2 and the other pure gas (H_2, CO_2, CH_4) permeation rates were measured by soap-bubble flow meter. The permeation experiment was carried out at 523 K and at 0.15-0.35 MPa absolute on the feed side.

Separation performance of gas mixture was evaluated by the separation factor, $\alpha_{i/j}$, defined by the following equation.

$$\alpha_{i/j} = \frac{y_i/y_j}{x_i/x_j} \qquad (4)$$

where x_i (or x_j) and y_i (or y_j) are the molar fractions of the component i (or j) in the feed and permeated gas, respectively.

2.4 Reaction experiment

Reaction experiment was carried out with the conditions as follows: reaction temperature 623 – 973 K, molar ratio of H_2O to CH_4 1 : 3, gas feed rate 100 – 300 Nml/min, superficial space velocity 0.08 - 0.4 s⁻¹, reaction pressure 0.2 MPa absolute. The permeation rate of the product gas was measured by the same method used for the gas permeation experiment. The compositions of the gas mixture of the feed and permeated gas were determined by the gas chromatography.

3. Experimental Results and Discussions

3.1 Performance of ZrO_2/SiO_2 composite membrane

Figure 4 shows the relationship between the

pure gas permeation fluxes of H_2, CO_2, CH_4 and H_2O through the ZrO_2/SiO_2 composite membrane and trans-membrane pressure at 523 K. Fluxes through the membrane. Permeation fluxes for each gas increase linearly with the increase of the trans-membrane pressure. The permeances of each gas are defined by the each slope of the relationships in Fig. 4. The main permeation mechanism for all the gases tested except H_2O was estimated as Knudsen diffusion, while that for H_2O was estimated as surface diffusion[4]. The permeances of H_2, CH_4 and CO_2 through this membrane were showed on Table 3. Figure 5 shows the relationship between separation factor of gaseous mixture of CH_4-CO_2 and trans-membrane pressure at 298 K. Applying the equation of Present-de Bethune[8] to this relationship, the average mean pore diameter of the membrane was estimated about 4nm.
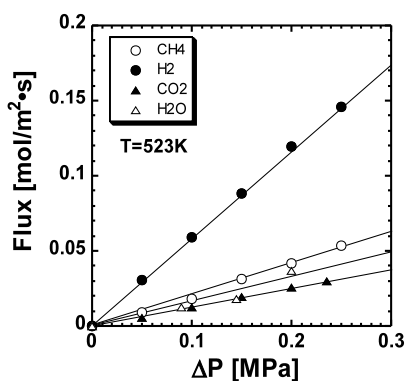
Table 3. Permeance through ZrO_2/SiO_2 membrane

H_2	5.9 x 10^{-7} [mol/(m^2 Pa s)]
CH_4	2.1 x 10^{-7} [mol/(m^2 Pa s)]
CO_2	1.3 x 10^{-7} [mol/(m^2 Pa s)]

3.2 Performance of Pd membrane

The theoretical permeation flux through Pd membrane J_{H2} [mol/(m^2s)] was defined by the following equation[9],

$$J_{H2} = k e^{(-E/RT)}(P_H^{0.5} - P_L^{0.5})　\qquad (5)$$

where P_H and P_L are pressures of the feed and permeation sides, respectively.

Figures 6 and 7 show the effects of pressure and temperature on the obtained permeation flux, respectively. Both linear relationships in these graphs indicated that the flux mechanism through this Pd membrane satisfied the equation (5).
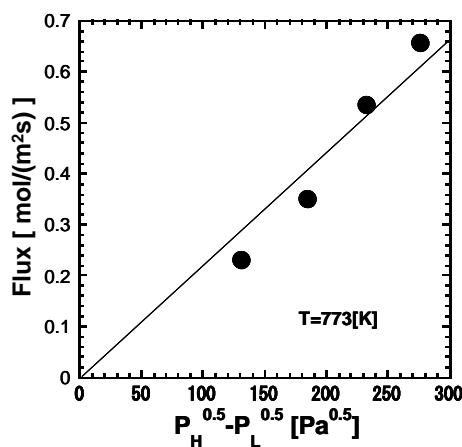

Fig. 4. Relationship between flux and trans-membrane pressure
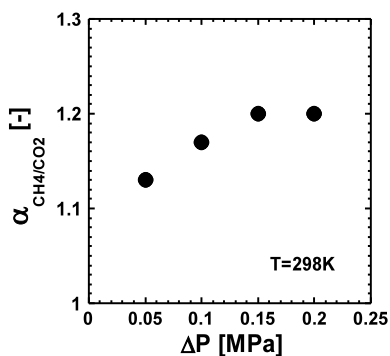
Fig. 5. Relationship between separation factor and trans-membrane pressure.

Fig. 6. Relationship between flux of H_2 through a palladium membrane and $P_H^{0.5}$-$P_L^{0.5}$.

The permeances of H_2 and He through this Pd membrane were showed on Table 4. These results showed the prepared Pd membrane is a high hydrogen-permselective dense membrane as the permeance of H_2 was 65 times that of He.
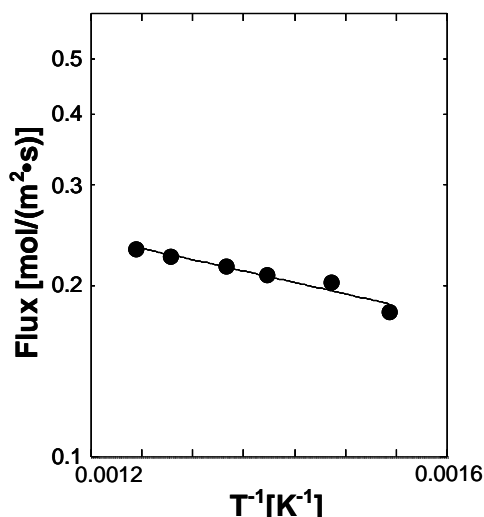
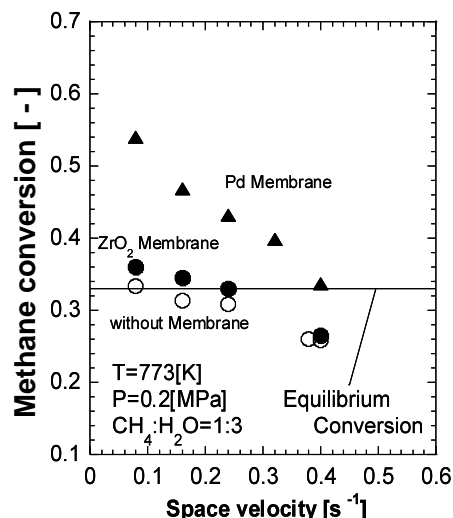Fig. 7. Arrhenius plot between the hydrogen permeation flux and temperature

Fig. 8. Relationship between space velocity and conversion

Table 4. Permeance through Pd membrane

H_2	3.06×10^{-6} [mol/(m^2 Pa s)]
He	4.72×10^{-8} [mol/(m^2 Pa s)]

3.3 Membrane reactor test

Figures 8 and 9 show the effect of space velocity and temperature on the methane conversion for three reactors, without membrane, with the ZrO_2/SiO_2 composite membrane, and with Pd membrane, respectively. Both figure solid lines are indicated the equilibrium conversion for each given condition, respectively.

In Fig. 8 the methane conversions for the reactors installed the hydrogen perm-selective membrane became greater than the equilibrium conversion in the case of the ZrO_2/SiO_2 composite membrane and the Pd membrane below the space velocity of 0.2 s^{-1} and 0.4 s^{-1}, respectively, though that for the reactor without membrane could reach the ewuilibrium conversion below the space velocity of 0.08 s^{-1}. In Fig. 9 the methane conversion for the both membrane reactors was shown to be greater than the equilibrium conversion in the all tested temperature range.
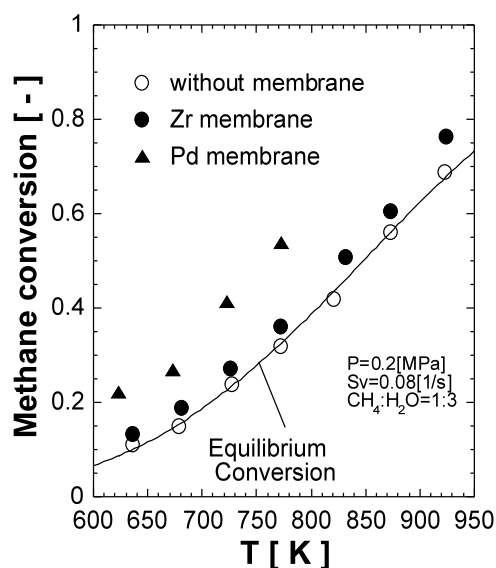

Fig. 9. Relationship between temperature and conversion

4. Numerical Analysis

4.1 Reactor model

The schematic diagram of the systems with and without separation membrane are shown in Fig. 10 (a) and (b), respectively.

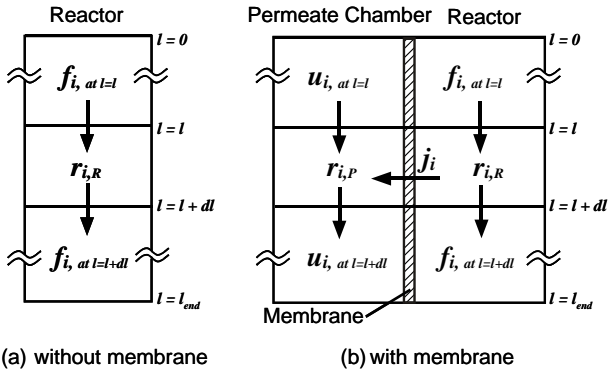(a) without membrane　　　(b) with membrane

Fig. 10. Schematic diagram of Reactor for numerical analysis

The plug flow in the reactor and permeate chamber, uniform temperature in the each chamber and no concentration gradient in the vertical direction to the flow are assumed. Material balances of each gaseous component across a longitudinal length, dl of the reactor yields the following ordinary differential equations. More detail derivation of the equations and the numerical integration method were described in the previous papers [10-12].

(Conventional Reactor)

$$\frac{d(f_i \cdot s_R)}{dl} = s_R \cdot v_i \cdot r_{CH_4} \qquad (6)$$

(Membrane Reactor)

(In the main chamber (reactor))

$$\frac{d(f_i \cdot s_R)}{dl} = s_R \cdot v_i \cdot r_{CH_4,R} - \frac{s_R}{h} \cdot j_i \qquad (7)$$

(In the permeate chamber)

$$\frac{d(u_i \cdot s_P)}{dl} = s_p \cdot v_i \cdot r_{CH_4,P} + \frac{s_R}{h} \cdot j_i \qquad (8)$$

where f_i [mol/s] (or u_i [mol/s]), v_i [-], and j_i [mol/(m²s)]are the flow rate, the stoichiometric coefficient, the permeation flux of component i, respectively, s_R [m²], s_P [m²], and h [m]are the cross-sectional areas of reactor and permeate chamber and the volume ratio of reactor volume

to membrane area, respectively, and $r_{CH_4,R}$ [mol/(m³ s)] and $r_{CH_4,P}$ [mol/(m³ s)]are the reaction rates of methane in reactor and permeate chamber, respectively[13].

Figures 11 and 12 show the results of the simulation[6] using the numerical analysis. Figures 11 and 12 correspond to Figs 8 and 9, respectively. As the calculated results agreed with the experimental data, the numerical analysis was thought to be adequate at the given conditions.

The mole fraction profile in the reactor at 773 K and 0.08 s⁻¹ of the space velocity is shown in Fig. 13. The drastic change at 0.05 m of reactor length indicates the position of separation membrane.
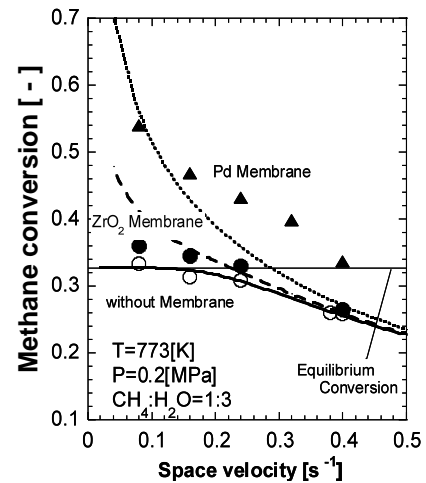

Fig. 11. Relationship between space velocity and conversion
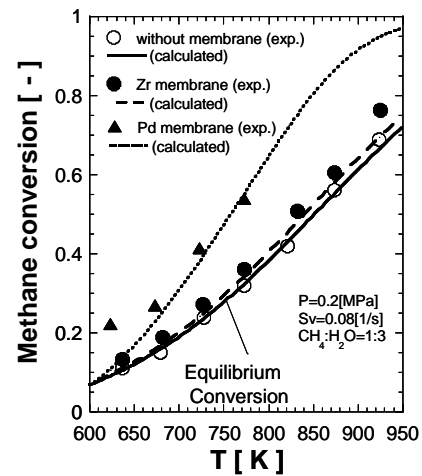

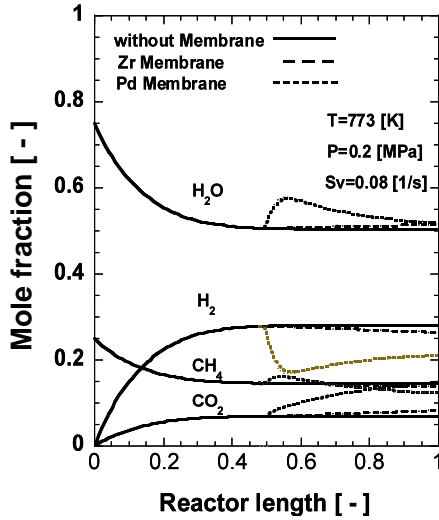Fig. 12. Relationship between temperature and conversion

Fig. 13. Mole fraction profile in reactor

4.2 Exergy analysis

To consider hydrogen as the secondary energy, the required energy to obtain hydrogen needs to be evaluated on a reasonable basis. In this study the evaluation method was proposed to compare quantitatively between the obtained exergy of product and the total exergy supplied in the reaction system.

The exergy of mixture is the sum of the following exergies, the sum of the chemical exergy E_0, the sum of the exergy due to temperature change E_T, the exergy due to compression E_P, the sum of the exergy due to mixing E_M. Each exergy is defined by the following equations[14],

$$E = E_0 + E_T + E_P + E_M \qquad (10)$$

$$E_0 = \sum n_i e_i^0 \qquad (11)$$

$$E_T = \left(\sum n_i C_{P,i} \right) \int_{T_0}^{T} \left(1 - \frac{T_0}{T} \right) dT \qquad (12)$$

$$E_P = NRT_0 \int_{P_0}^{P} \left(\frac{1}{P} - \frac{P_0}{P^2} \right) dP \qquad (13)$$

$$E_M = NRT_0 \sum x_i \ln(x_i) \qquad (14),$$

where n_i [kmol], e_i^0 [kJ/kmol], x_i [-] and $C_{p,i}$ [kJ/(kmolK)] are number of moles, standard chemical exergy, mole fraction and heat capacity at constant pressure of component i, respectively, and N [kmol] and R [kJ/(kmol K)] are total number of moles and gas constant, respectively.

The exergy of each system was calculated by using these equations on the base of flow schemes[14-16] in Fig.14. On the supposition of ideal heat input and output, the exergy loss of each system was evaluated by converting to the basis per one mole product hydrogen.
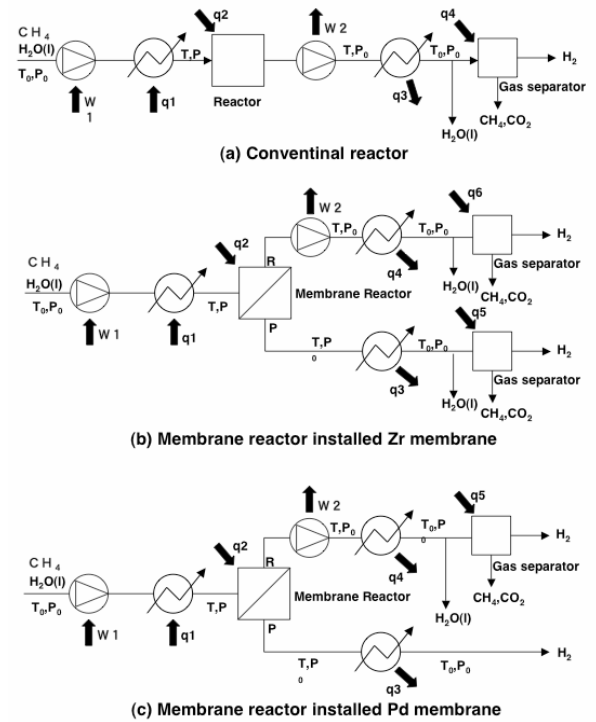

Fig. 14.　　Process flow diagram for exergy analysis

The relationship between temperature and the exergy loss per mol hydrogen production is shown in Fig. 15. The exergy loss decreases rapidly with a temperature rise in the lower range, while the decreasing becomes gentle in the higher range. Compare with the exergy loss for the conventional reactor without membrane, that for the membrane reactor installed the ZrO_2/SiO_2 composite membrane and the Pd membrane in was saved $5 - 10$ % and $30 - 50$%, respectively.
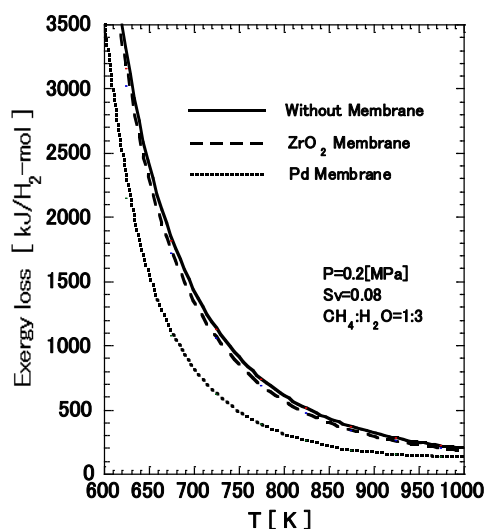
Fig. 15. Relationship between temperature and exergy loss based on the value at 773K without membrane

5. Conclusions

(1) Two types of hydrogen-permselective membranes, ZrO_2/SiO_2 composite membrane and Pd membrane with high hydrogen-selectivity could be formed on a porous ceramic tube.

(2) The membrane reactors installed hydrogen-permselective membrane in were constructed, methane steam reforming reaction was carried out using the membrane reactors, and higher conversion of methane for membrane reactor than that for the conventional reactor was obtained.

(3) Theoretical equations for membrane reactor were applied to analyze the experimental data of methane conversion.

(4) Effectiveness of membrane reactor was showed by the numerical analysis in exergy saving.

References

1. Itoh, N., AIChE Journal vol.33, p1576-1578(1987)

2. Uemiya, S., Sato, N., Ando, H., Matsuda, T., Kikuchi, E., Applied Catalysis, Vol.67, p223-230(1990)

3. Uemiya, S., Sato, N., Ando, H., Kikuchi, E., Ind. Eng. Chem. Res., vol.30 p585-589(1991)

4. Ohya, H., Nakajima, H., Togami, N., Aihara, M., Negishi, Y., J. Membrane Sci., vol.97, p91-98(1994)

5. Shu, J., Grandjean, B. P. A., Ghali, E., Kaliaguine, S., J. Membrane Sci., vol.77, p181-195(1993)

6. Uemiya, S., Matsuda, T., Kikuchi, E., J. Membrane Sci., vol.56,p.315-325(1991)

7. Uemiya, S., Matsuda, T. Kikuchi, E., Nippon Kagaku Kaishi (6), p669-675(1990)

8. Present, R. D., Debethune, A. J., Phys. Rev., vol.75, p1050(1991)

9. Yan, S., Maeda, H., Kusakabe, K., Morooka, S., Ind. Eng. Chem. Res., vol.33, p.616-622(1994)

10. Ohashi, H., Ohya, H., Aihara, M., Negishi, Y., Semenova., S. I., J. Membrane Sci., vol.146, p39-52(1998)

11. Fan, J., Ohya, H., Ohashi, H., Aihara, M., Takeuchi, T., Negishi., Y., Semenova, S. I., J. Membrane Sci., vol.162, p125-134(1999)

12. Ohashi, H., Ohya, H., Aihara, M., Takeuchi, T., Negishi., Y., Fan, J., Semenova, S. I., J. Membrane Sci., vol.166, p239-247(2000)

13. Lunde, P. J., Kester, F. L., J. Catalysis, vol.30, p423-429(1973)

14. Yoshida, K., "Ekuserugi Kogaku," Kyoritsu Shuppan, p154(1999).

15. Hinderink, A. P., Kerkhof, F. P. J. M., Lie, A. B. K., Arons J. D. S., Kooi, H. J. V. D., Chem. Eng. Sci., vol.51(20), p4693-4700 (1996)

16. Inagaki, Y., Haga, K., Aita, H., Sekita, K., Koiso, H., Hino, R., Nihon Genshiryoku Gakkaishi, vol.40(1), p59-64(1998)